JAMES RENNIE BEQUEST

REPORT ON EXPEDITION/PROJECT/CONFERENCE

Expedition/Project/Conference Title: Lab Placement: Mapping the Interaction between Ammodytoxin C and its known substrates.....

Travel Dates: 15th July-15th Sep.....

Location: Ljubljana, Slovenia.....

Group Member(s): Carla Clark .....

Aims: Mapping the Interaction between Ammodytoxin C and its known substrates.....

OUTCOME (not less than 300 words):-

I would like to thank Dr. Igor Krizaj for allowing me to work at the Joseph Stefan Institute. I would also like to thank Lidija Kovacic my mentor for much appreciated help and guidance. A further thanks to Dr Jim Allan and those granting the James Rennie Bequest, for making my stay in Slovenia possible. Bellow is my final report from the summers work.

Mapping the interaction between ammodytoxin C and its substrates.

1. INTRODUCTION

Phospholipases A_2 (PLA_2s) are a superfamily of diverse enzymes that catalyze the hydrolysis of the *sn*-2 ester bond of phospholipids. Their known functions are many and varied, including involvement in inflammation, cell injury, tumour resistance and neurotoxicity. Ammodytoxins (Atxs) A, B, and C are group IIA sPLA2s with presynaptic neurotoxicity, isolated from the venom of the long-nosed viper (*Vipera ammodytes ammodytes*)[1]. Presynaptically acting sPLA2 neurotoxins interfere specifically with the release of acetylcholine from motorneurons, and their PLA2 activity is essential for the irreversible blockade of neuromuscular transmission[2]. Electron microscopy studies of a β-neurotoxin-paralysed neuro-muscular junction, reveals a depletion of the neurotransmitter-containing synaptic vesicles (SV) in the nerve terminal. And suggests that the retrieval of SV from the plasma membrane is impaired[3]. However, the molecular mechanism of presynaptic $sPLA_2$ toxicity is still not completely understood. Both enzymatic activity of $sPLA_2$ toxins[3]. and their specific binding to proteins are believed to be involved in the process. One such toxin, ammodytoxin C, has been shown to bind protein disulphide isomerase (PDI), Calmodullin (CaM) and 14-3-3 proteins[4]. To study the specific interaction of AtxC with these proteins a chemical cross-linker, sulpho-SBED, was used to link and isolate interacting peptide regions of toxin and substrate. Based on this interaction map, a model for the CaM-AtxC interaction was composed. Furthermore, these mapped interactions allow for suggestions as to their involvement in neorotoxicity.

2. MATERIALS AND METHODS

2.1. Chemicals

AtxC was purified from *Vipera a. ammodytes* venom as described (Gubenšek et al., 1980). Sulfo-SBED reagent (sulfosuccinimidyl-2-[6-(biotinamido)-2-(pazidobenzamido) hexanoamido] ethyl-1,3'-dithiopropionate), disuccinimidyl suberate (DSS), monomeric avidin gel and streptavidin linked to horseradish peroxidase (SAHRP) were from Pierce (USA). The substrate to measure the phospholipase activity was prepared from 1-hexadecanoyl-2-(1-pyrenedecanoyl)-*sn*-glycero-3-phosphoglycerol (PyrPG) (Molecular Probes, USA). 14-3-3 proteins were isolated as described[5]. Recombinant yeast PDI was a gift from Dr. William J. Lennarz, State University of New York at Stony Brook, USA[6]**.** BM Chemiluminescence Western Blotting Kit was from Roche Diagnostics (Switzerland).

2.2. Synthesis of sulfo-SBED-AtxC

One mg of sulfo-SBED was dissolved in 50 µL DMSO immediately before use. AtxC was dissolved in water at 1 mg/mL and mixed with the sulfo-SBED at room temperature in molar ratios AtxC to sulfo-SBED of 1 : 1.1. Reaction mixtures were stirred for 30 minutes and then dialyzed overnight against 50 mM Hepes/HCl, pH 7.3, 150 mM NaCl to remove excess sulfo-SBED and small molecular mass side products (cut off 10 kDa). The resulting solution was aliquoted and frozen at -80 °C. All manipulations were performed in the dark.

2.3. Labeling of soluble AtxC-binding proteins with sulfo-SBED-AtxC

Sulfo-SBED-AtxC was mixed with PDI or 14-3-3, each in the labeltransfer buffer (75 mM Hepes/HCl, pH 8.2, 150 mM NaCl and 2 mM $CaCl_2$ – final volume 1500 µL) and incubated at room temperature for 60 minutes in the dark. The molar

ratios between the photoprobe preparation and PDI or 14-3-3 proteins were in 1:1 molar ratios. After incubation, the mixtures were placed on ice and irradiated by five 15 W UV lamps at 312 nm at a distance of 5 cm, for

2.4. Isolation of biotinylated peptides

Conjugates were cleaved using chemotrypsin (2% chemotrypsin (w/w of protein)) three times, for 30 min at 37ºC. Avidin gel (100µl) was regenerated by washing in an eppendorf tube: four times with LTB, four times with BB/EB, six times with 0.1% TFA and four times
with LTB; centrifuging for 2 min at 9000Xg to separated gel from solution between each step. Seperately, each conjugate was added to the gel and mixed for 2 hrs at room temperature or 4ºC overnight. The gel was then washed four times with LTB and five times with ddH20, centrifuged as with gel preparation and breakthrough collected. Biotinylated proteins were eluted by addition of 200µl of 0.1% TFA and centrifuged as above and the eluate collected. The elution procedure was repeated three times.

2.5 Amino terminal protein sequence analysis

Prior to sequencing, cleaved conjugate, avidin gel breakthrough and avidin gel eluate were desalted by HPLC separately on a Chrompack reversed-phase C18 column (100×3.0mm) equilibriated with 0.1% TFA and eluted by 90% acetonitril with 0.1% TFA (solution B). The flow rate was 1ml/min, with absorbance monitored at 215nm and solution B applied to the column to the following program:

Program Time	% of Buffer B
0	0
5	0
35	60
47	100
52	100
53	0
56	0

Peptides from the avidin gel eluate were collected between 15-30 min of program time (between 20%-54% of buffer B) and lyophilized before subjecting to automated Edman degredation sequencing. An Applied Biosystems liquid-pulsed protein sequencer 475A, on-line connected to a phenylthiohydantoin-amino acid analyzer 20A of the same manufacturer was used.

2.5. SDS Page analysis

Samples of uncleaved conjugate, cleaved conjugate, avidin gel breakthrough and avidin gel eluate were analyzed on SDS-PAGE (12.5% acrylamide gels) in both reducing buffer (0.5% (m/v) NaDs, 10% (m/v) glycerol, 50 mM DTT, 0.25% (m/v) bromophenol blue and 32 mM Tris; pH 6.8) and non-reducing buffer (0.5% (m/v) NaDs, 10% (m/v) glycerol, 0.25% (m/v) bromophenol blue and 32 mM Tris; pH 6.8). Samples were boiled for 5 min prior to loading on the gel along with pre-stained standards. Electrophoresis was performed in running buffer (0.1% (m/v) NaDS, 192 mM glycine, 25 mM Tris/HCl; pH 8.3) in a Mighty small SE 260 (Hoefer, ZDA), 20mA per gel.

2.6. Western Blotting

Following running SDS-PAGE electrophoresis, the gel was washed for 15 min in KP buffer (12.2 mM K_2HPO_4, 7.8 mM KH_2PO_4, pH 7). Two pieces of BioRad 3mm filter paper, one piece of PVDF membrane (14-3-3 proteins) or nitrocellulose membrane (PDI) were cut to the exact size of the gel. Filter paper was soaked in KP buffer and membranes were pre-treated by soaking in 100% methanol for 1 min, washing with water and transferring to KP buffer. The filter paper was placed on the negative side of the holder, the gel was placed on its surface, and the corresponding membrane on top of the gel

and the remaining piece of filter paper was placed on the membrane. The holder was closed as a sandwich and placed in a BioRad blotting tank with KP buffer. Electrophoresis was run for 90min at 200mA.

2.7. Detection of biotinylated proteins on membranes

The membranes from the electrophoretic blocks were incubated for 1hr in 1% blocking solution (w/v) in TBS (50 mM Tris, 150 mM NaCl, pH 7.5) to block non-specific binding sites. Then they were incubated for 30min with streptavidin conjugated to horse radish peroxidase in TBS and membranes were then washed for 15min, four times in TBST buffer (Tween 20 0.1% (v/v)). To start the chemiluminesence reaction, detection solution was then added according to the manufacturer's instructions. Immediately, the membranes were exposed on Kodak BioMax Light Film (Sigma-Aldrich, USA) for 60 sec and then developed.

2.8. Mapping interaction to 3D-structures

Files containing atomic co-ordinates for CaM, PDI and BMH2 (PRB ID: 1CLL[7]; 2B5E[6]; 2BR9 respectively) were obtained from http://www.pdb.org and those for AtxA were obtained from a model[8]. Within these files all hetero-atoms were removed, except for Ca2+ atoms in CaM, and in the case of AtxA all disulphide bonds were inputed. CaM-AtxA docking was then performed using three programs: ClusPro programs DOT and ZDOCK[9] and Global Range Molecular Matching - X (GRAMM-X)[10]. All solutions were viewed in Pymol[11] and possible solutions were selected by referring to sequences from their mapped interaction. Hex 4.5[12] (http://www.csd.abdn.ac.uk/hex) was then used with the possible complex solution to improve energies and eliminate clashes and the most probable solution selected.

2.9 Measuring the affect of CaM on AtxC PLA_2 activity

The phospholipase activities of AtxC and AtxC-CaM were compared using the modified method of Radvanji et al (1989). Activity was assayed in 50mM KCl, 1mM $CaCl_2$, 50mM Tris/HCl; pH 7.4 buffer, supplemented with 0.06% (w/v) fatty-acid free bovine serum albumin and using fluorogenic PyrPG phospholipid vesicles (1.4 µM final concentration) as substrate. Fluorescence was measured in a 96-well plate on a SAFIRE microplate monochromator reader (Tecan, Austria) in 10 kinetic cycles at λ_{ex} 342nm, λ_{em} 395nm with 10 flashes and an integration time of 40 µs. All measurements were performed in triplicate**.** Background fluorescence was measured in control experiments lacking AtxC and subtracted from the experimental curves.

2. RESULTS AND DISCUSSION

2.1 Isolation of biotinylated peptides

Sulfo-SBED is used as a trifunctional label transfer reagent used to study protein-protein interactions. AtxC was attatched to Sulfo-SBED via its amine-reactive group as a 'bait' protein and incubated with PDI or BMH2 as 'prey'. The bait:prey complex was captured by stimulation of the photoreactive group to covalently link to the complexed prey protein. The resultant conjugates were cleaved and regions containing the biotin moiety from the Sulfo-SBED cross-linker were isolated via the affinity between biotin and avidin immobilized in gel. Upon reduction of this complex, the biotin label that first resided with the bait protein, AtxC transfers to the prey protein, PDI or BMH2. By detection on Western Blots, the biotin was further utilized to determine if the isolation was efficacious. For both AtxC-BMH2 and AtxC-PDI the isolation was successful as only the gel eluate contained biotinylated peptides and the breakthrough did not; therefore no biotynylated peptides were lost during their isolation. Peptides containing biotin can be those involved directly in the AtxC-PDI/BMH2 interaction, however, will also include those found neighboring the site of the interaction. This is due to the tight association of amino acids at the binding site, making binding of proteins to sulfo-SBED-AtxC more difficult in this region. Supposing this occurs adjacent amino acids, not directly involved in binding, AtxC may be in close

enough proximity to the toxin (~ 15 Å) for binding to the cross-linker, following UV irradiation. Thus it should be considered that those peptides define the binding site and not solely those regions directly involved in binding.

2.2 Sequence analysis

Chromatograms from the separation of peptides of cleaved conjugates, avidin gel breakthrough and eluate were compared in order to select peptides for sequencing. It was imperative that only peptides involved in protein-protein interactions were selected and consequently must be bound to biotin. Therefore those peptides evident in the cleaved conjugate as well as eluate, whilst absent from the breakthrough were chosen. When discerning the sequences of these peptides they had to conform with chemotrypsin cleavage sites, and for AtxC peptides they must also contain or be adjacent to residues containing amine groups (Lys/Arg) for binding with Sulfo-SBED. Furthermore longer and overlapping sequences were given presidence to prevent inclusion of ambiguous sequence.

2.3 Mapping PDI-AtxC interaction

With the protein samples chosen for sequencing there was substantial overlapping of sequence for both PDI and AtxC (Fig. 1), affirming three main regions of interaction on each Lys or Arg for cross-linker to bind. This discrepancy is likely due to the disulphide bond between Cys26 in the sequence and the C-terminal region involved in the interaction, allowing for this likely non-interacting sequences inclusion in those samples with the C-terminal end peptide. PDI is found in all eukaryotic organisms and tissues, with high sequence conservation allowing for generalized comparisons between yeast PDI and mammalian PDI. This high degree of conservation combined with the recent elucidation of yeast PDI's crystal structure[6] and numerous studies on PDI's functions have allowed for the inference of the physiological implications of the PDI-AtxC interaction.

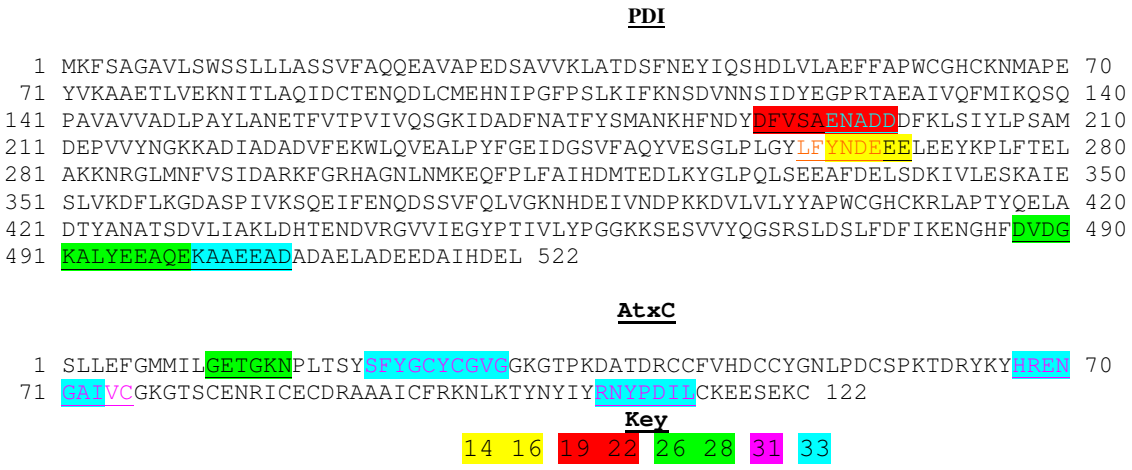

Fig. 1 Isolated peptides from AtxC-PDI interaction.
Sequences of those peptides involved in the AtxC-PDI interaction are underligned and highlighted corresponding to the HPLC fraction they were collected from. Fractions with continual overlap (e.g. 14 & 16) were designated as one to simplify results.

PDI has five main domains: a, b, a', b' and c; of which the a and a' domains contain the active sites, b and b' contain hydrophobic pockets for protein binding and the c domain being the C-terminal tail. Our results indicate that the three main regions of interaction with AtxC are applicable to the b, b' and c domains (Fig.2) This is in accordance with results from interaction of AtxC with PDI domain deletion mutants (Kovačič et al, 2006, data unpublished). In these studies, western blot analysis ascertained that toxin mainly binds the b and a'c domains. Whilst the b' domain does not show as strong binding as the b and a'c domains this can be explained by its implicated function. The b and b' domains contain hydrophobic pockets, which the crystal structure suggests is crutial for the interaction of PDI and substrates. From progressive truncation studies of both mammalian[13] and yeast PDI[6] it was concluded that the b' domain is the primary substrate binding site for the refolding of proteins in the ER. Contrastingly, from the interaction of folded AtxC and PDI mutants,

the b domain shows higher significance, presumably indicative of a role outside of the ER; an involvement in AtxC neurotoxicity.

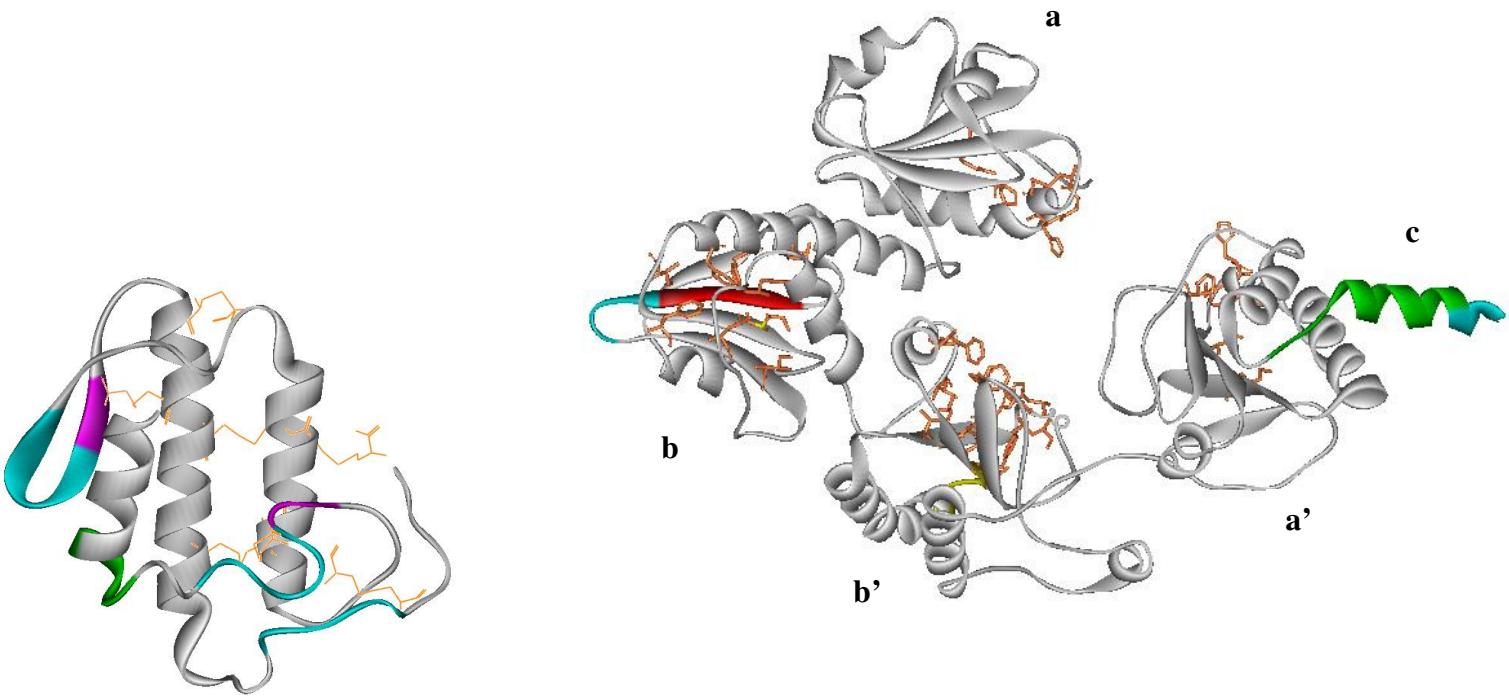

Fig. 2 PDI-AtxC Interaction mapped to primary and 3D structures
AtxC is to the left and PDI to the right. Colours correspond to the HPLC fraction the peptides came from . AtxC's disulphide bonds are highlighted in stick format in orange. PDI residues in orange depict putative hydrophobic residues for protein-protein interactions, AtxC can be seen to bind in regions b, b' near the hydrophobic pockets and c.

PDI's function as a chaperone and for the folding and formation of disulphide bonds of proteins in the ER has been well documented, however vast literature indicates PDI has other subcellular localizations with functions that differ from those displayed in the ER lumen. PDI has also been found in the nucleus and cytosol as well on the cell membrane and the extracellular matrix. Interestingly, on the extracellular surface of the plasma membrane reshuffling of disulphide bonds by PDI has been found to be essential for the internalization and exertion diphtheria toxin's effects[14], as well as the sinbid virus[15] and HIV[16] virus-cell fusion. With the observation that four cysteine residues are found in the PDI-interacting regions of AtxC this is probable. Furthermore, in platelets, blocking PDI with inhibitory antibodies inhibits a number of platelet activation pathways, including granule secretion[17] which is how AtxC brings about its neurotoxic effects; prevention of Ach secretion. Moreover, in this study PDI was found to be associated with integrin, with inhibition of PDI disrupting integrin function, one of which is neurotransmitter release at nerve terminals. Similarly, the extensive interaction between AtxC and PDI's C-terminal tail could be linked to PDI inhibition. The c-domain is engaged in hydrophobic interactions with the a' domain and has been proposed to stabalise the a' active site, corresponding with the requirement of the c-terminus for full PDI function[6]. Binding of AtxC to the c-domain could destabilize the ac' interaction; impairing the co-operative activity between active sites and consequently inhibiting PDI and preventing acetylcholine release. Thus PDI may be involved in the internalization of AtxC for internal exertion of neurotoxicity, or AtxC could inhibit PDI itself, disrupting secretion externally.

2.4 Mapping BMH2-AtxC interaction

The 14-3-3 proteins are a large family of approximately 30kDa acidic proteins which exist primarily as homo- and heterodimers within all eukaryotic cells. As with PDI, there is a high degree of sequence conservation between species and between all 14-3-3 isotypes, particularly in the regions which form the dimer interface or line the central ligand binding channel of the dimeric molecule.

Therefore BMH2 can be used as a general representation of all 14-3-3 proteins. Mapping the AtxC-BMH2 interaction revealed that the same three regions of toxin were involved as with PDI: the end of the N-terminal helix, the beta-sheet, and the c-terminal tail (bringing the peptide bound by a disulphide bond). Furthermore 14-3-3 proteins are known to bind phosphoryalated serine/threonines on target molecules. Using NetPhos 1.0 and phosphomotif finder putative phosphorylation sites were identified on AtxC, that were in the regions of interaction (Fig.3). However the importance of phosphorylation at these sites is still to be tested. Contrastingly, the sequences mapped to BMH2 were less conclusive, although were found to be in regions highly conserved between isotypes. This was as expected, as proteins binding to 14-3-3s appear to initially bind to a single dominant site and then subsequently to many, much weaker secondary interaction sites.

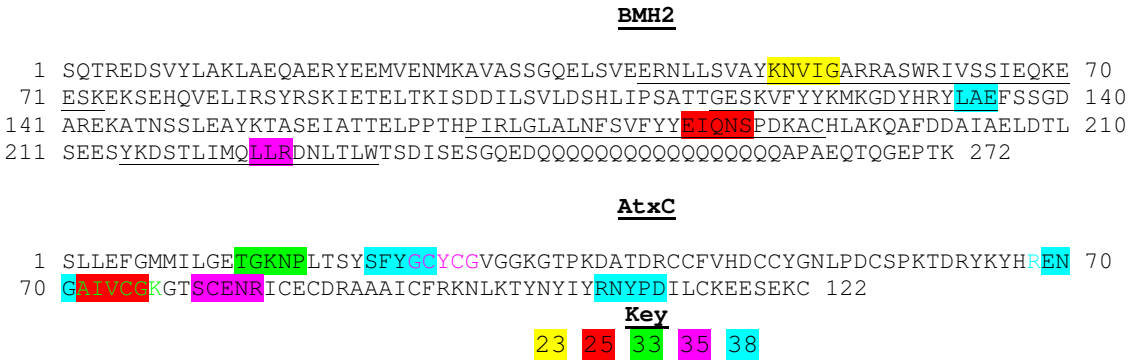

Fig.3 Isolated peptides from AtxC-BMH2 interaction.
Sequences of those peptides involved in the AtxC-PDI interaction are highlighted corresponding to the HPLC fraction they were collected from. Underlined BMH2 sequence indicates helices 3, 5, 7 and 9 respectively.

Each 14-3-3 protein sequence can be roughly divided into three sections: a divergent amino terminus, the conserved core region and a divergent carboxyl terminus. The conserved middle core region of the 14-3-3s encodes an amphipathic groove that forms the main functional domain. Four helices in each monomer (H3, H5, H7 and H9) form this concave amphipathic groove that interacts with target peptides. We propose that the dominant binding site is in this groove (Fig.4), although other binding sites may exist. As numerous proteins bind in this amphipathic groove, with a diverse array of functions, this gives little indication as to the consequences of the AtxC-BMH2 interaction. Although 14-3-3 proteins perform different functions for different ligands, generally actions include changes in the activity of bound ligands, altered association of bound ligands with other molecules, and the control of subcellular localization of the bound ligand. Wurtele *et al* (2003)[18] mapped the interaction between a fungal phytotoxin, fusicoccin, and a 14-3-3-H+ATP-ase regulatory complex. They found that toxin binding strengthened the association of the plasma membrane H+ATP-ase C-terminal end with 14-3-3, permanently activating the proton pump and thus producing fusicoccin's toxic effects. Interestingly, amino acids involved in the fusicoccin-14-3-3 interaction, correspond with those involved in the AtxC-14-3-3 interaction and PDI has been identified as a 14-3-3 binding protein[19]. Therefore it can be postulated that both toxins bind to 14-3-3 to alter a regulatory complex by a similar mechanism: altering interactions with the C-terminal tail of the bound ligand, resulting in toxicity. Evidently, fungal toxin interaction occurs at plant plasma membranes and not mammalian neuronal membranes. However, 14-3-3 proteins have been identified as having many functional roles in secretion and catelcholamine release[19].

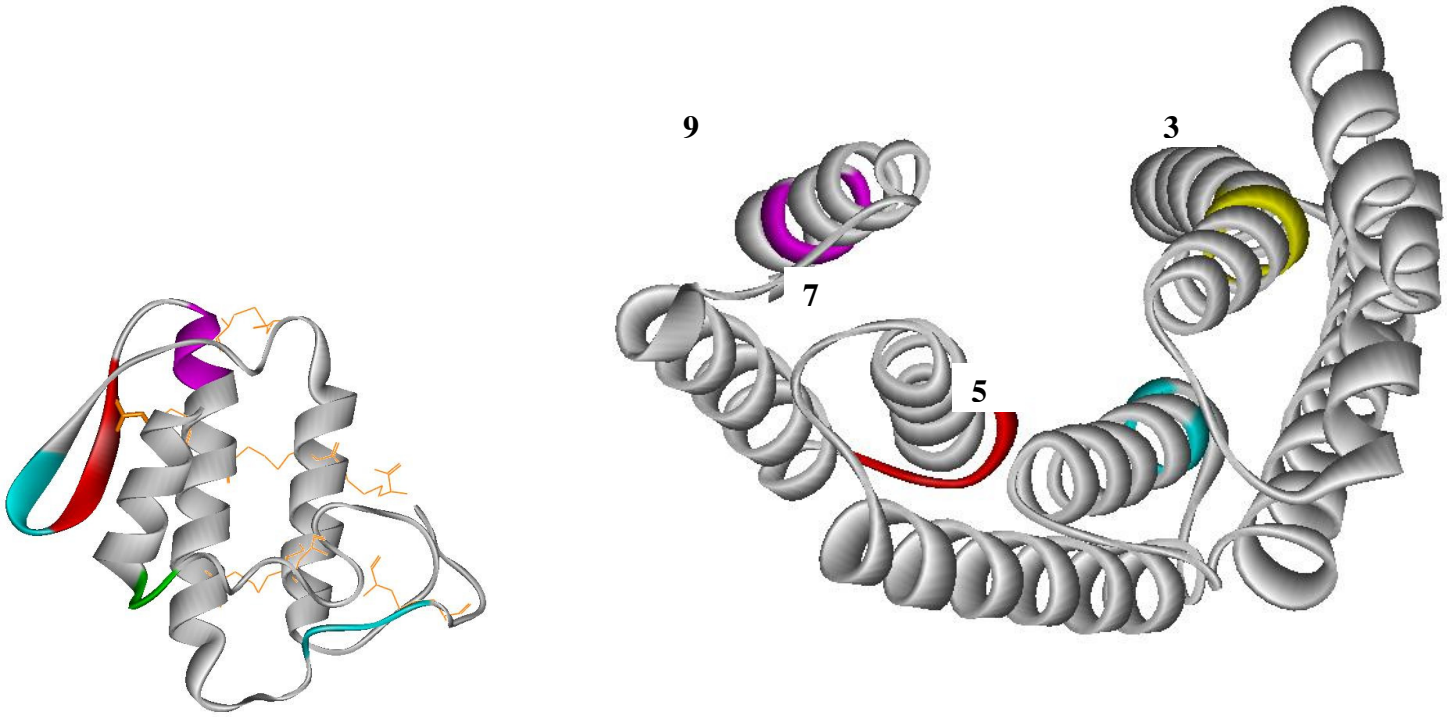

Fig.4 Sites of interaction between AtxC-BMH2
Atxc is to the left and BMH2 to the right. Colours correspond to the HPLC fraction the peptides came from. AtxC's disulphide bridges are shown in stick form in orange. The four helices forming the amphiphatic binding groove are labeled accordingly.

In yeast, altered expression of BMH2 resulted in a loss of targeted vesicle transport to the plasma membrane, possibly attributable to breakdown of the actin cytoskeleton, but was clearly indicative of a blockade of a signaling pathway required for secretion, possibly the MAP kinase pathway[20]. In adrenal chromaffin cells, 14-3-3 mediated Ca2+ dependent exocytosis was enhanced by protein kinase C interactions, via phosphorylation with another unidentified component in the exocytosis machinery[22]. More significantly, phosphorylation of a component of the presynaptic active zone, Rim, a modulator of exocytosis was required for binding of 14-3-3s[22], which where also found to be necessary for neurotransmitter release in Drosophila. Outwith roles in actin skeleton reorganization, it has also been suggested that 14-3-3s may have a more distinct effect on membrane fusion, and the γ isoform was found as an extrinsic membrane protein and in granules, and could bind aggregate phospholipids and thus may modify phospholipids for exocytosis[23]. If AtxC was to affect 14-3-3s actions in this instance, it is likely that its pharmological effects would be dependant on enzymatic activity; the hydrolysis of phospholipids. As a consequence of the myriad of 14-3-3 binding proteins it is possible that ammodytoxin could affect any of the afformentioned interactions, and it should also be noted that the specific cell type and 14-3-3 isoform will affect the 14-3-3s predominant role.

2.5 CaM-AtxC interaction

Sequences from CaM-AtxC interaction mapping had previously been acquired (Kovačič et al, 2006, data unpublished) and have been aligned with the full sequences of CaM and AtxC (Fig.5). Using the Calmudulin Target Base motif finder a putative binding domain was found that correlates with the interaction at the C-terminal end (Fig.5). For the central region of interaction on the toxin no binding motifs were identified, however, upstream of this sight 1-8-14, 1-5-10 and 1-16 hydrophobic motifs were found. Similarly, 1-8-14, 1-14 and 1-16 hydophobic CaM binding motifs were found at the N-terminal end interaction site, providing a strong basis from which to find a model of the interaction. AtxC's phospholipase activity, a requirement for toxcicity, is Ca2+ dependent[2] and thus the structure of CaM with Ca2+ bound was used for docking. Initially the programs DOT, ZDOCK and GRAMM-X were used to for CaM-AtxC docking. GRAMMX was used due to its Fast Fourier Transformation (FFT) algorithm refined by employing smoothed potentials, refinement stage, and knowledge-based scoring. Similarly DOT and ZDOCK programs also use an FFT algorithm, with evaluation based on shape complementarity, desolvation energy, and

electrostatics; and rank docking conformations based on their clustering properties. With ZDOCK results are filtered further to improve the energies and eliminate clashes, and then the electrostatic and desolvation energies are recomputed. Resulting conformations showing alignment of the regions of interaction were then given to Hex, which, unlike other docking programs uses polar Fourier correlations to accelerate docking calculations giving a refined range of possibilities with the most compatible energies.

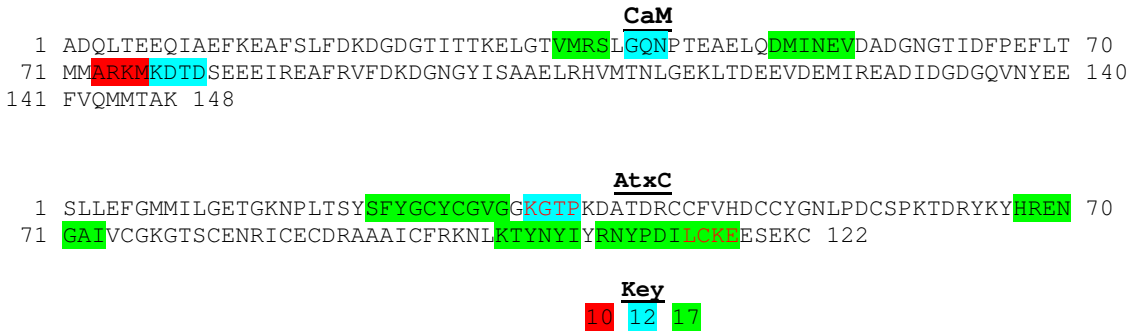

Fig.5 Isolated peptides from AtxC-CaM interaction.
Sequences of those peptides involved in the AtxC-CaM interaction are underligned and highlighted corresponding to the HPLC fraction they were collected from.

To select the most probable models, a number of conditions were considered.
By comparing the phospholipase activities of AtxC and AtxC-CaM it was shown that CaM increased the activity significantly (Kovačič et al, 2006, data unpublished). Therefore in the models, AtxCs enzymatic active site should not be masked by CaM. A narrow hydrophobic pocket extends into the active site, of which His 47 (His 48 in AtxA) is important for activity[7]. Models one and two, those with the lowest complex energies, were disregarded as access to this hydrophobic pocket was restricted. Contrastingly, in all other solutions the active site was more accessable, making them more likely candidates. Of these models, the two with the lowest conformational energies, models 3 and 4, conformed with distances for the crosslinker to link interacting regions (Fig.6A). The interaction between toxin and CaM was extensive in both models. There were four hydrogen bonds found between AtxC and CaM in each model (Fig.6B), with variations in the amino acids involved, yet the bonds are in similar regions. In both instances the toxins c-terminal tail is involved in three hydrogen bonds; one at the CaMs N-terminal lobe (Helix 3 with model 3 and helix 2 with model 4), and two bonds with the central alpha-helix. The last bond is between CaM's c-terminal lobe and helix 2 (model 3) or helix 3 (model 4) of toxin. Of particular significance is the bond between the end of AtxC's c-terminal tail and the central helix, which is between the same residues in both models. In all the models the basic c-terminal tail of AtxC interacts with the more acidic central alpha-helix of CaM further strengthening this interactions relevance. The c-terminal tail is also involved in hydrophobic interactions with the n-terminal lobe (Fig.6C). Phe 113 of the toxin fits into a hydrophobic pocket, which is more extensive in model 4, involving five residues rather than three. From the docking it is evident that the c-terminal tail is the predominant region for the interaction with CaM, which has also been suggested with AtxA for binding with both CaM and R25[24]. Furthermore the c-terminal region has been demonstrated to be of importance for neuroxicity, particularly with both hydrophobic/aromatic and basic residues[8]. With the CaM interaction we have also found that with the exception of Tyr107 in a hydrogen bond in model 3, only hydrophobic/aromatic and basic residues are involved, strengthening the possibility that CaM is involved in neurotoxicity.

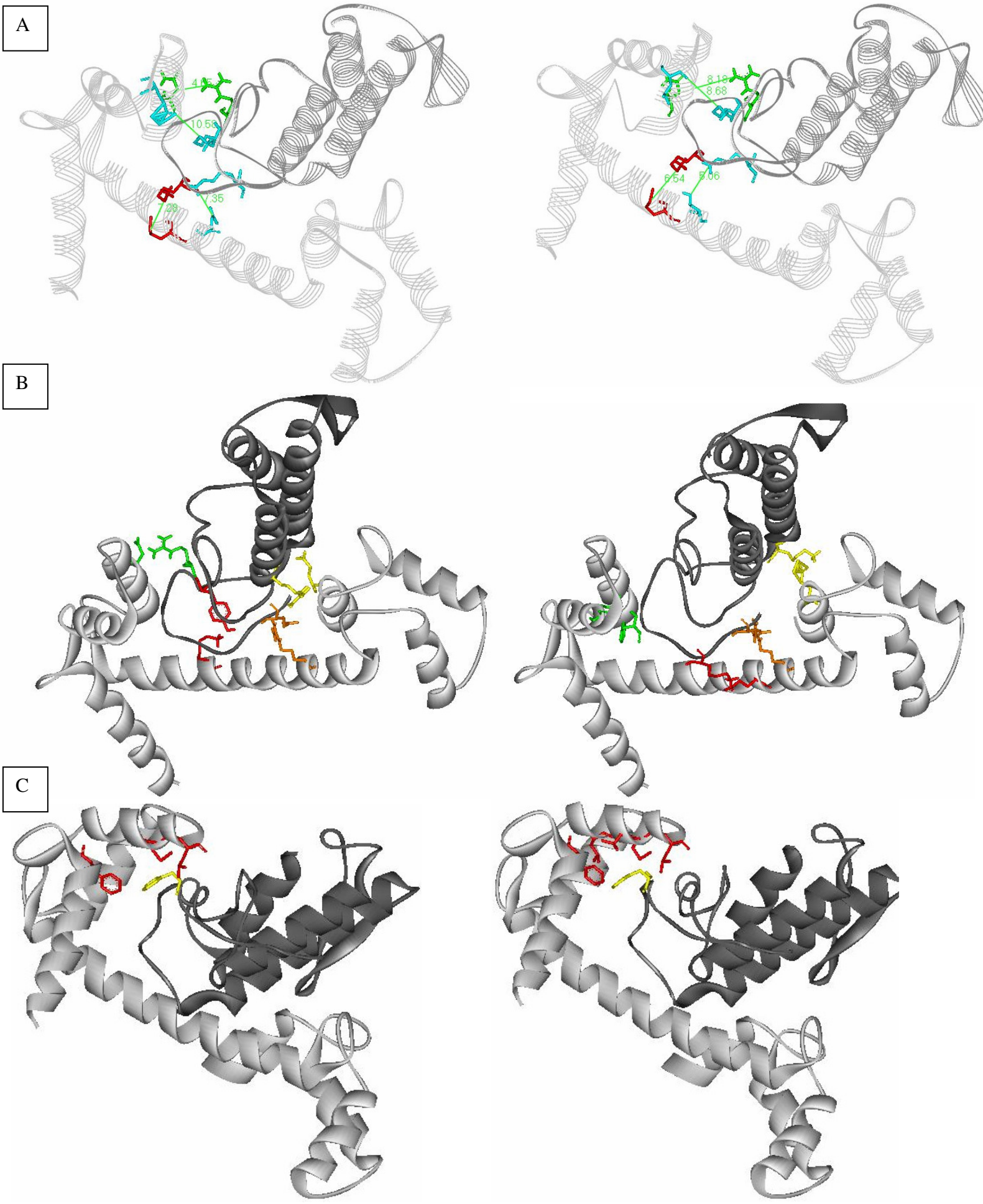
A
10.58
7.35
8.18
8.68
B
C

Fig.6 Cross linking, Hydrogen bond and hydrophobic interaction comparison of model 3 and 4
Diagrams on the left correspond with model 3 and those on the right model 4. Toxin is in dark grey and CaM is in light grey. A) Cross-linking distance comparison. Model 3 distances (Å): green residues, blue residues, red residues. Model 4 distances (Å): green residues, blue residues, red residues. Colours are those assigned to HPLC fractions as in Fig 5. B) Hydrogen bond comparison. Similarly coloured residues are H-bonded. C) Comparison of hydrophobic interaction.

Despite the evidence for model 3 and 4 as representations of the complex, the structure of CaM changes drastically without Ca2+ ions bound and these models would be ineffectual. Although AtxC's phospholipase activity, is Ca2+ dependent this may not be linked with CaM. By highlighting those regions involved in the interaction with Ca2+ free CaM it can be seen if binding to toxin is possible in this state (Fig.8). Whilst two of the mapped regions are within a reasonable distance from each other, the third is on the same lobe but at the other side of the molecule, and thus it is physically improbable that toxin binds to calcium free CaM. Furthermore those amino acids involved in electrostatic and hydrophobic interactions have different orientations or become internalized and grouped together making them unavailable for interaction. As Ca2+ is required for AtxC to bind CaM as well as for neurotoxicity, it seems probable that the requisites for calcium are linked: CaM in the presence of Ca2+ is a component of the neurotoxicity pathway.

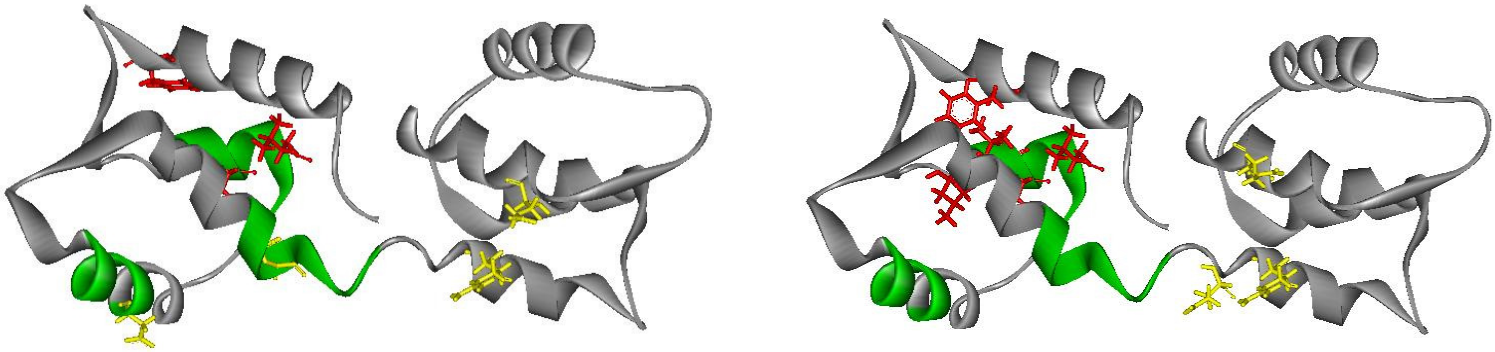

Fig.8 Ca2+ free CaM and mapped interactions.
Diagrams on the left correspond with model 3 and those on the right model 4. Isolated peptides involved in the AtxC interaction are labeled green., hydrophobic pocket residues are red and H-bonding residues are yellow.

3. CONCLUSIONS

In all three interactions AtxC was found to interact via an N-terminal region, a central region and its C-terminal region. With PDI, AtxC interacts at different predominant binding regions to that of non-native protein substrates indicative of a role outwith protein folding in the ER lumen. Functional studies on PDI's largely uncharacterized c domain, may shed light on the consequences of this AtxC interaction. Concerning, BMH2, interactions were mapped to its amphiphatic groove, the main functional region, however other binding sites are likely to exist. Whether this interaction is phosphorylation dependent, as with other 14-3-3 substrates is still to be ascertained. The CaM-AtxC complex models represented show hydrogen bonding with AtxC via its N-terminal Lobe, C-terminal lobe and central alpha-helix, and hydrophobic interactions with an extensive hydrophobic pocket at its N-terminal lobe. Furthermore this interaction is Ca^{2+} dependent as AtxC cannot bind Ca^{2+}-free form. Models of PDI-AtxC and BMH2-AtxC are currently underway and should shed light on the molecular mechanisms of AtxC neurotoxicity. Moreover continual studies that aid the elucidation of these mechanisms will undoubtedly be important to our understanding of the mechanisms involved in nerve transmission.

4. REFERENCES

1) Thouin, L. G., Ritonja, A., Gubensˇek, F., and Russell, F. E. (1982) Neuromuscular and lethal effects of phospholipase A from *Vipera ammodytes* venom, *Toxicon* ***20***, 1051-1058.

2) Gubenšek, F., Pattabhiraman, T.T. and Russel, F.E. (1980) Phospholipase A_2 activity of some crotalid snake venoms and fractions. *Toxicon* **18**, 699-701.

3) Montecucco and Rossetto, O. (2000) How do presynaptic PLA_2 neurotoxins block nerve terminals? *Trends Biochem. Sci.* **25**, 266–270

4) Sribar, J., Copic, A., Poljsak-Prijatelj, M., Logonder, U., Gubensek, F. And Krizaj, I. (2003) R25 is an intracellular membrane receptor for a snake venom secretory phospholipase A. *FEBBS Lett.* **553,** 309-314.

5) Šribar, J., Sherman, N.E., Prijatelj, P., Faure, G., Gubenšek, F., Fox, J.W., Aitken, A., Pungerčar, J. and Križaj, I. (2003). The neurotoxic phospholipase A_2 associates, through a non-phosphorylated binding motif, with 14-3-3 protein γ and ε isoforms. *Biochem. Biophzs. Res. Commun.* **302**, 691-696.

6) Tian, G., Xiang, S., Niova, R., Lennarz, W.J., Schindelin, H., (2006) The crystal structure of yeast protein disulphide isomerase suggests cooperativity between its active sites. *Cell* **124**, 61-73.

7) Chattopadhyaya, R., Meador, W.E., Means, A.R., Quiocho, F.A. (1992) Calmodulin structure refined at 1.7A resolution. *J. Mol. Biol.* **288**, 1177-1192.

8) Pungerčar, J., Križaj, I., Liang, N.-S. & Gubenšek, F. (1999) An aromatic, but not basic, residue is involved in the toxicity of group-II phospholipase A_2 neurotoxins. *Biochem. J.* **341**, 139-145.

9) Comeau, S.R., Gatchell, D.W., Vajda, S. and Camacho, C.J. (2004) Clus Pro: an automated docking and discrimination method for the prediction of protein complexes. *Bioinformatic* **20**, 45-50.

10) Tovchigrechko, A. and Vakser, I.A. (2006) GRAMM-X public server for protein-protein docking. *Nucleic Acids Res.* **34**, W310-4)

11) DeLano, W.L. (2002) The PyMOL Molecular Graphics System. *http://www.pymol.org*

12) Mustard, D. and Ritchie, D.W. (2005) Docking essential dynamics eigenstructures. *Struct. Funct. Genet.* **60**. 269-274.

13) Darby, N.J., Van Straaten, M., Penka, E., Vincentelli, R. and Kemmink, J. (1999) Identifying and characterizing a second structural domain of protein disulfide isomerase. *FEBS Lett.* **448**, 167-172.

14) Mandel, R., Ryser, H.J., Ghani, F., Wu, M. and Peak, D. (1993) Inhibition of a Reductive Function of the Plasma Membrane by Bacitracin and Antibodies Against Protein Disulfide-Isomerase. *Proc. Nat. Acad. Sci*. **90**, 4112-4116.

15) Abell, B.A. and Brown, D.T. (1993). Sindbis virus membrane fusion is mediated by reduction of glycoprotein disulfide bridges at the cell surface. *J. Virol.* **67,** 5496-5501.

16) Ryser, H.J., Levy, E.M., Mandel, R. and DiSciullo, G.J. (1994) Inhibition of Human Immunodeficiency Virus Infection by Agents that Interfere with Thiol-Disulfide Interchange Upon Virus-Receptor Interaction. Proc. Nat. Acad. Sci. **91,** 4559-4563.

17) Jordan, P.A., Stevens, J.M., Hubbard, G.P., Barret, N.E., Sage, T., Authi, K.S. and Gibbins, J.M. (2005). A role for the thiol isomerase protein ERP5 in platelet function. *Blood.* **105,** 1500-1507.

18) Wurtele, M., Jelich-Ottmann, C., Wittinghofer, A. and Oecking, C. (2003). Structural view of a fungal toxin acting on a 14-3-3 regulatory complex. *EMBO J.* **22,** 987-994.

19) Pozuelo Rubio, M., Geraghty, K.M., Wong, B.H., Wood, N.T., Campbell, D.G., Morrice, N. and Mackintosh, C. (2004) 14-3-3-affinity purification of over 200 human phosphoproteins reveals new links to regulation of cellular metabolism, proliferation and trafficking. *Biochem. J.* **379,** 395-408.

20) Roth, D., Birkenfield, J. and Betz, H. (1999). Dominant-negative alleles of 14-3-3 proteins cause defects in actin organization and vesicle targeting in the yeast Saccharomyces cerevisiae. *FEBS Lett.* **460,** 411-416.

21) Morgan, A. and Burgoyne, R.D. (1992) Interaction between protein kinase C and Exo1 (14-3-3 protein) and its relevance to exocytosis in permeabilized adrenal chromaffin cells. *Biochem J.* **286**, 807-811.

22) Sun, L., Bittner, M.A. and Holz, R.W. (2003) RIM, a component of the presynaptic active zone and modulator of exocytosis, binds 14-3-3 through its N-terminus. *J. Biol. Chem.* **278,** 38301-38309.

23) Roth, D., Morgan, A., Martin, H., Jones, D., Martens, GJ., Aitken, A. and Burgoyne, R.D. (1994) Characterization of 14-3-3 proteins in adrenal chromaffin cells and demonstration of isoform-specific phospholipid binding. *Biochem. J.* **301,** 305-310.

24) Prijatelj, P., Sribar, J., Ivanovski, G., Krizaj, I., Gubensek, F. and Pungercar, J. (2003) Identification of a novel binding site for calmodulin in ammodytoxin A, a neurotoxic group IIA phospholipase A2. *FEBS.* **270,** 3018-3025.